Entangled Photon Spectroscopy

Emma Berger

April 2, 2021

Abstract

Entangled photon spectroscopy is an exciting new technology in chemistry, materials science, and biology that utilizes quantum light to gain control over excited state populations, maximize signal enhancement, and study the quantum nature of complicated systems. A background on entangled photons, light-matter interactions, and nonlinear spectroscopy is provided first. This framework is used to demonstrate entangled light's ability to selectively control excitonic distributions in a model system. Applications in chemistry and materials science are explored, which include photosynthetic systems, fundamental coherent reaction dynamics, and chiral molecules. Examples of possible future directions in the field are proposed, with particular emphasis on experiment.

1 Introduction

Entanglement is a curious feature of quantum mechanics for which there is no classical counterpart. It is a phenomenon that results in a many-body system when the quantum state cannot be described by a direct product of each of the constituent element's states. Instead, it is represented mathematically by a superposition state, in which the properties of the individual particles are highly correlated and are undetermined until a measurement process "collapses" the entangled state (Figure 1).

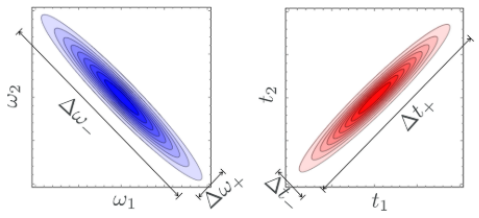

Figure 1: Entangled photons exhibit strong energy-time correlations. The frequencies of the two photons ω_1, ω_2 are strongly anticorrelated, while their arrival times t_1, t_2 are strongly correlated. Reprinted from [1].

Entangled states of light have been used extensively in physics since the 1950s for testing fundamental aspects of quantum mechanics. Additionally, they have generated much interest in the quantum information, for applications ranging from quantum computing, quantum communication, and quantum cryptography, to name a few. However, the use of quantum light as a probe for chemical systems is a largely unexplored area. The birth of entangled photon spectroscopy is marked around 1990, when several groups around the world, including Rarity and colleagues, demonstrated the generation of energy entangled photons from a parametric down-conversion process [2]. After senidng 827 nm entangled photon pairs into a single Mach-Zehnder interferometer, they observed nonclassical oscillations in the coincidence rate of photon counts for path length differences both smaller and larger than the single photon coherence length. This was exciting for physical chemists, who began investigating how entangled light could serve as a spectroscopic tool to uncover new chemical phenomena.

Quantum states of light naturally have distinct intensity fluctuations, a nonclassical bandwidth, and correlations between different degrees of freedom. Entangled photon spectroscopy capitalizes on these properties to probe chemical systems with enhanced signal and control over excitation pathways. Whereas classical correlations are basis dependent, entangled light exhibits strong correlations in any basis. What this means is that entangled light can have strong time and frequency correlations, for example, while classical light can only have one of the two [1].

Another unique feature of entangled photons is their light-matter interaction, which scales linearly with input intensity at low photon fluxes, rather than quadratically as would be expected classically [3]. This can be understood by imagining a three state system with a ground, intermediate, and excited state. With classical light, the probability of a two-photon absorption process leading to population in the excited state is proportional to the product of the probability of being in the intermediate state and the transition rate from the intermediate to excited states. Both of these factors are proportional to the intensity of light, thus leading to an I^2 dependence. On the other hand, if we assume a low enough light intensity, the two photons come from the same pair. As a result, there is a linear scaling in the two-photon absorption signal for entangled light. This principle is particularly exciting for chemists, as it enables the study of photosensitive and biological samples that would otherwise require intensities of classical light above their damage thresholds.

Such two-photon absorption experiments form the basis of entangled photon spectroscopy. How can we understand these types of experiements? In typical two photon coincidence measurements, the probability that both detectors click is described by the $G^{(2)}$ correlation function introduced by Glauber:

$$\begin{aligned} G^{(2)}(t) = \eta^2 \int_{-t_w/2}^{t_w/2} d\tau \, \langle\psi| \, \hat{a}_1^\dagger(t)\hat{a}_2^\dagger(\tau+t) \\ \hat{a}_2(\tau+t)\hat{a}_1(\tau)\,|\psi\rangle \\ = \eta^2 f(t) t_w A_{d1} A_{d2} \Phi + ... \end{aligned}$$

where η is the detector efficiency, t_w is the detector window, the ladder operators are for a specific mode of the electromagnetic field, A_{di} is the area of the i^{th} detector, f(t) is a time-dependent factor,Φ is the photon flux density, and the second equality is derived elsewhere [1]. In an entangled photon spectroscopy experiment, the two detectors are replaced by the sample. The rate of two-photon absorption at low photon fluxes is

$$R_{\mathrm{TPA}} \propto f(p_f(t))$$

where $p_f(t)$ is the probability of being in the two-photon excited state and is a function of convoluted 4-point matter and field correlation functions. It is this convolution of field and matter that is the hallmark of entangled photon spectroscopy and allows control over population dynamics and distributions. A more in-depth derivation will be provided below.

This text is outlined as follows: sections 2 and 3 provide background on the light-matter interaction Hamiltonian and nonlinear spectroscopy following the tutorial in [4], section 4 describes how entangled photon pairs are generated experimentally, section 5 discusses two particular applications of entangled photon spectroscopy, and section 6 provides a conclusion and outlook for the field.

2 The Light-Matter Interaction Hamiltonian

Within the dipole approximation, we can write the light-matter Hamiltonian as

$$H_{\mathrm{dip}} = \sum_n H_n + \frac{\epsilon_0}{2}\int (\vec{E}^2 + c^2\vec{B}^2) d^3\vec{r} - \sum_n \hat{\mu}_n \vec{E}(\vec{r}_n) \tag{1}$$

The first term in equation (1) describes the n^{th} molecular Hamiltonian

$$H_n = \sum_k \epsilon_{\mathrm{nk}} \, |nk\rangle \, \langle nk| \tag{2}$$

where the index k denotes the k^{th} energy level on the n^{th} molecule. The second term in equation (1) is the free-space field Hamiltonian with the electric and magnetic field operators denoted $\vec{E}$ and $\vec{B}$, respectively. The third term in equation (1) describes the field-matter coupling, where

$$\hat{\mu}_n = -eq_n \tag{3}$$

is the dipole moment of the nth molecule with charge e and position q, and

$$\vec{E}(z,t) = i\hat{e}\int d\omega \sqrt{\frac{\hbar\omega}{4\pi\epsilon_0 cA}} e^{i\omega(z/c-t)} a(\omega) \tag{4}$$

is the electric field operator with polarization unit vector $\hat{e}$. The continuous raising and lowering operators $a(\omega)$ and $a^\dagger(\omega)$ for the mode of frequency ω obey the commutation relations $[a(\omega), a^\dagger(\omega')] = \delta(\omega - \omega')$. Second order perturbation theory can be used to find the eigenstates for equation (1) by treating the uncoupled terms as H_0 and the light-matter coupling term as H_1. Excitations in the resultant delocalized eigenstates are called excitons. Deriving this approach in its entirety is beyond the scope of this paper, but the following result is important to note. In the limit that the light-matter interaction is weak, we can write the time-varying dipole operator as

$$\hat{\mu}_n(t) = \vec{V}_n(t) + \vec{V}_n^\dagger(t) \tag{5}$$

where

$$\vec{V}_n(t) = \mu_n b_n e^{-i\omega t} \tag{6}$$

$$\vec{V}_n^\dagger(t) = \mu_n b_n^\dagger e^{i\omega t} \tag{7}$$

describe excitations between the delocalized exciton states through the b_n and $b_n^\dagger$ ladder operators. Invoking the rotating wave and slowly varying envelope approximations results in a light-matter interaction term of the form

$$\boxed{H_{\mathrm{int}}(t) = \sum_n \vec{V}_n(t)\vec{E}^\dagger(t) + \vec{V}_n^\dagger(t)\vec{E}(t)} \tag{8}$$

where the electric field terms that describe the creation and annhiliation of photons are given as

$$\vec{E}(t) = i\hat{e}\sqrt{\frac{\hbar\omega_o}{4\pi\epsilon_0 cA}}\vec{a}(t) \tag{9}$$

$$\vec{E}^\dagger(t) = -i\hat{e}\sqrt{\frac{\hbar\omega_o}{4\pi\epsilon_0 cA}}\vec{a}^\dagger(t) \tag{10}$$

It is this interaction Hamiltonian (equation 8) which will be the subject of study in the upcoming sections.

3 Measuring Observables of $H_{\text{int}}(t)$ with Nonlinear Spectroscopy

We imagine a real experiment where a sample of molecules is excited by quantum light and the details of the light-matter interaction are extracted with a photon counting experiment. What we'd like to do is quantitatively predict what the signal will be. To begin, we start with some background on applying nonlinear optics to $H_{\text{int}}(t)$ under the simple assumption that the sample contains only a single molecule. Equation 8 then becomes:

$$H_{\text{int}}(t) = \vec{V}_n(t)\vec{E}^\dagger(t) + \vec{V}_n^\dagger(t)\vec{E}(t) \tag{11}$$

We can write this in the interaction picture as

$$H_{\text{int}}^I(t) = e^{iH_0\tau/\hbar} H_{\text{int}}(t) e^{-iH_0\tau/\hbar} \tag{12}$$

where H_0 is the uncoupled part of the overall Hamiltonian from equation (1). Let's define the contracted notation

$$H_{\text{int},-}^I(t)X = H_{\text{int}}^I(t)X - XH_{\text{int}}^I(t) \tag{13}$$

The density matrix $\rho(t)$ describing the time evolution of the system is then

$$\boxed{\rho(t) = \mathcal{T}\exp\left[\frac{i}{\hbar}\int_{t_0}^{t} d\tau H_{\text{int,-}}^I(t)\right]\rho(t_0)} \tag{14}$$

where $\mathcal{T}$ is the time-ordering operator and $\rho(t_0)$ is the initial state of the system. To calculate nonlinear optical signals, equation (14) is expanded as a Taylor series and $\rho(t)$ will have field-matter correlations as a result of $H_{\text{int}}^I(t)$.

With this formalism, we can define the initial state of the system as $\rho(t_0) = |g(t_0)\rangle\langle g(t_0)| \otimes \rho_{\text{field}}(t_0)$ where the matter and field are both in their ground states. We wish to quantify some observable that we will measure. The observable will be a function of ladder operators of the electromagnetic field, since any spectroscopy experiment measures the change in photons after the light-matter interaction compared to the number incident on the system. With this, the observable is:

$$\mathcal{O}(t) = f(\{a_i^\dagger(t)\}\{a_j(t)\}) \tag{15}$$

where i and j indicate different modes of the field. In any experiment, we measure average values of observables. By definition:

$$\langle\mathcal{O}\rangle = \int_{-\infty}^{\infty} dt\ \text{tr}\{\mathcal{O}(t)\rho(t)\} \tag{16}$$

If we set $\langle\mathcal{O}\rangle_{t=0} = 0$, then what's measured is the relative change in this observable. Plugging in equations (12, 14, 16) allows calculation of the measured signal S for any arbitrary observable

$$\begin{aligned} S = &\frac{i}{\hbar}\int_{-\infty}^{\infty} dt \int_{t_0}^{t} d\tau [\langle [\mathcal{O}(t), E(\tau)]_+ V_+^\dagger(\tau)\rangle \\ &+ \langle [\mathcal{O}(t), E^\dagger(\tau)]_+ V_+(\tau)\rangle] \end{aligned} \tag{17}$$

where $\langle ... \rangle$ is the average over $\rho(t)$ and where $(AX)_\pm = AX \pm XA$ is a shorthand notation.

Suppose our observable is a fluorescence signal in which $\mathcal{O}(t) = \hat{a}^\dagger(t)\hat{a}(t)$. This should make intuitive sense because fluoresence involves the absorption of a photon (subtraction of photon from the field), followed by emission of a photon (gain of photon into the field). Using our interaction Hamltonian, Taylor expanding the signal, equation (17), to second order, and neglecting any terms that involve lowering operators on ground states of the field and matter terms of $\rho(t)$, assuming no photons begin in the mode in which photons are emitted, leaves us with a final result in the real part of the signal (to second order) of

$$\begin{aligned} S^{(2)} \propto &\int_{-\infty}^{\infty} dt \int_{t_0}^{t} d\tau \langle V(t)V(\tau)V^\dagger(\tau)V^\dagger(t)\rangle \\ &\langle E^\dagger(t)E^\dagger(\tau)E(\tau)E(t)\rangle \end{aligned} \tag{18}$$

What we see is that the signal involves the convolution of 4-point matter and 4-field correlation functions, which will capture quantum correlations. This is where quantum spectroscopy can yield interesting results. In general, the n^{th} order correlation function of the sample is connected to that of the field in the measured signal.

4 Generating Time-Energy Entangled Photon Pairs

The most common process by which entangled photons are generated is type-II spontaneous degenerate parametric down conversion. In general, PDC is a process by which a pump photon of frequency ω_p incident on a birefrigent crystal with a $\chi^{(2)}$ nonlinearity generates two photons of frequencies ω_a and ω_b, called the signal and idler photons [5]. Degenerate type-II PDC is where the signal and idler photons have the same energy and orthogonal polarizations. In a material with a $\chi^{(2)}$ nonlinearity, the polarization in the material can be expanded in powers of the electric field. The second-order response in a PDC process is

$$\hat{H}^{(2)} = \epsilon_0 \int_V d^3\vec{r}\chi_{ijk}^{(2)}\hat{E}_i\hat{E}_j\hat{E}_k \tag{19}$$

where the electric field operators are

$$\hat{E}(\vec{r},t) = \int d^3\vec{k}[\hat{E}^{(-)}(\vec{k})e^{-i(\omega t-\vec{k}\cdot\vec{r})} + \hat{E}^{(+)}(\vec{k})e^{i(\omega t-\vec{k}\cdot\vec{r})}] \tag{20}$$

and where

$$\hat{E}^{(-)}(\vec{k}) = i\sqrt{\frac{2\pi\hbar\omega(\vec{k})}{V}}\hat{a}^\dagger(\vec{k}) \tag{21}$$

$$\hat{E}^{(+)}(\vec{k}) = i\sqrt{\frac{2\pi\hbar\omega(\vec{k})}{V}}\hat{a}(\vec{k}) \tag{22}$$

Substituting equations (20-22) into equation (19), retaining only the terms in which the signal and idler modes are initially in the vacuum state, gives a new Hamiltonian of the form

$$\hat{H}^{(2)} \sim \chi^{(2)}\hat{a}_p\hat{a}_s^\dagger\hat{a}_i^\dagger + \text{h.c.} \tag{23}$$

corresponding to the destruction of the pump photon and the creation of signal and idler photons. If the initial state of the light field prior to the PDC is $|\psi_0\rangle$, then the resultant state of the field after the PDC process is $|\psi\rangle = |\psi_0\rangle + |\psi_1\rangle$ where

$$|\psi_1\rangle = N\int d^3\vec{k}_s \int d^3\vec{k}_i \delta(\omega_p-\omega_s-\omega_i) \delta(\vec{k}_p-\vec{k}_s-\vec{k}_i)\hat{a}_s^\dagger\hat{a}_i^\dagger \tag{24}$$

Note that the resulting delta functions imply conservation of energy and momentum of the signal and idler photons. In type-II PDC, momentum conservation causes the signal and idler photons to be emitted from the nonlinear material in two intersecting cones. If a screen with pinholes is placed such that the signal and idler photons are selected from the points where the cones intersect, then one can generate time-energy entangled photons (Figure 2).

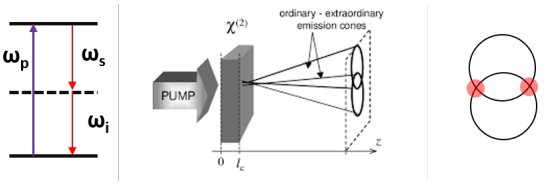

Figure 2: (left) In a type-II PDC process, a pump photon of frequency ω_p is passed through a nonlinear medium generating signal and idler photons of frequencies ω_s and ω_i, respectively. (middle) The daughter photons exit a $\chi^{(2)}$ medium of length l. Due to momentum conservation, they are emitted in two intersecting cones of different polarization. (right) By placing pinholes where the two cones intersect (red areas), one can select only entangled photon pairs.

If we call $|V\rangle$ and $|H\rangle$ the vertically and horizontally polarized single photon states emitted at the red points where the cones intersect, the corresponding state of the emitted light is

$$|\psi(t)\rangle = e^{-iHt/\hbar}|\psi_0\rangle \tag{25}$$

where

$$|\psi_0\rangle = |0\rangle_{Vs}|0\rangle_{Hs}|0\rangle_{Vi}|0\rangle_{Hi} \tag{26}$$

and where

$$H = \eta\hbar(\hat{a}_{Vs}^\dagger\hat{a}_{Hi}^\dagger + \hat{a}_{Hs}^\dagger\hat{a}_{Vi}^\dagger) + \text{h.c.} \tag{27}$$

$$\eta \propto \chi^{(2)}\mathcal{E}_p \tag{28}$$

where $\mathcal{E}_p$ is the undepleted amplitude of the pump pulse. Solving for the resultant state of the type-II PDC process yields

$$|\psi(t)\rangle = (1-\mu^2/2)|0\rangle_s|0\rangle_i - i\mu(|V\rangle_s|H\rangle_i + |H\rangle_s|V\rangle_i \tag{29}$$

where

$$\mu = \eta t \tag{30}$$

$$|0\rangle = |0\rangle_V|0\rangle_H \tag{31}$$

$$|V\rangle = |1\rangle_V|0\rangle_H \tag{32}$$

$$|H\rangle = |0\rangle_V|1\rangle_H \tag{33}$$

The important result of equation (29) shows that type-II PDC produces a quantum state of light in which the polarization, frequency, and time of the generated photons are entangled. Their energies are entangled due to conservation of energy: the sum of energies of the two daughter photons are determined by the energy of the pump photon. The daughter photons are therefore said to be "anticorrelated" in frequency. The times at which they exit the nonlinear crystal are entangled because they must be generated at the same time and only pick up relative time delays due to the nonzero refractive index of the nonlinear medium.

5 Applications of Entangled Light

5.1 Controlling Excited State Populations with Entangled Light

Theoretical investigations have shown that entangled photons can serve as an indispensible tool in the investigation of complex exciton dynamics due to the ability to selectively excite certain excitonic states that may be hard to populate otherwise. To understand this, we consider a simple excitonic ground state that is dipole-coupled to two single-exciton states $|e_1\rangle$ and $|e_2\rangle$, which are in turn coupled to two

separate two-exciton excited states $|f_1\rangle$ and $|f_2\rangle$ (Figure 3) [4].

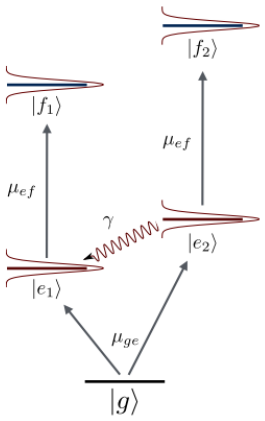

Figure 3: An imagined energy level diagram. The ground state $|g\rangle$ is coupled two single-exciton excited states $|e_1\rangle$ and $|e_2\rangle$ through a dipole moment μ_{ge}. The single-exciton states are in turn coupled to double-exciton excited states $|f_1\rangle$ and $|f_2\rangle$ through a dipole moment μ_{ef}. Decoherence interactions with the environment can cause the state $|e_2\rangle$ to relax to $|e_1\rangle$ with a rate of γ. Reprinted from [4]

If, however, state $|e_2\rangle$ couples to the environment incoherently and relaxes to state $|e_1\rangle$ on an ultrafast timescale, then classical spectroscopic investigations of $|f_2\rangle$ would be difficult because significant population of $|f_2\rangle$ is hindered by this environmental coupling process. To study the dynamics of this hypothetical system, two criteria need to be met. Firstly, minimal bandwidth in an exciation pulse is needed to populate $|f_2\rangle$ without accidentally populating $|f_1\rangle$. Secondly, to efficiently populate $|f_2\rangle$, the decay channel from $|e_2\rangle$ to $|e_1\rangle$ needs to be suppressed. This requires a two-photon absorption process in which the window of time between arrival of the two photons is faster than the decay channel.

Meeting both of these criteria is challenging for classical light pulses due to the lower bound on uncertainties the Heisenberg uncertainty relation $\Delta\omega\Delta t \geq 1$ imposes. However, entangled light produced from type-II PDC need not obey this relationship since the energy and time correlations of the two photons come from independent sources. That is, the bandwidth of the pump pulse limits the bandwidths of the signal and idler pulses, but the different group velocities of the signal and idler photons within the birefringent crystal set the entanglement time T, which determines the time delay between the two emitted photons. As such, time and frequency are no longer Fourier conjugate variables.

Applying equation (18) to this two-photon fluorescence experiment (the derivation of which is provided elsewhere [4]) yields a signal

$$S = \sum_f |\mu_{ef}|^2 \int dt\, p_f(t) \tag{34}$$

where the summation over f denotes 6 different paths $p_f(t)$ to the final state $|f_2\rangle$. The important result can be seen in figure 4.

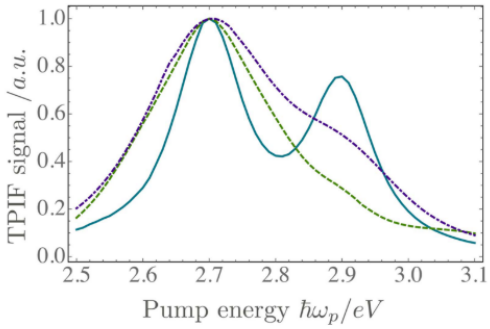

Figure 4: Two-photon fluorescence with entangled light incident on the system described by figure 3 results in the emission spectrum described by the solid teal line. Note that both double-exciton states are clearly resolved. Classical light incident on the sample with comparable frequency correlations (dashed green) and bandwidth (dashed purple) is not able to resolve the $|f_2\rangle$ state so clearly. Reprinted from [4].

With entangled light, the resultant energy spectrum is given by the blue line. Classical laser pulses incident on this system with comparable frequency resolution (green, dashed) or bandwidth (purple, dashed) are shown as well. The excited state $|f_2\rangle$ at 2.9 eV is clearly resolved in the case of entangled light, whereas it only appears as a shoulder off of the peak corresponding to $|f_1\rangle$ at 2.7 eV in the case of classical light. While this experiment was only hypothetical, it illustrates the power of entangled photons to selectively excite particular states that may be hard to populate with classical light.

The principle of selectively exciting double-exciton states is of particular interest for the study of energy transport processes in photosynthetic proteins. Previous experiments have shown that photosynthetic complexes form manifolds of single- $|e_i\rangle$ and two-exciton states $|f_i\rangle$ [6]. The mechanism by which photosynthetic proteins achieve such high quantum efficiencies is thought to result from the complex couplings between these states. However, the broad bandwidth of ultrashort laser pulses has made it challenging to control exciton distributions, resulting in complicated spectra with many overlapping features.

For example, $|f_i\rangle$ states may be accessible via several single-exciton channels due to single-exciton couplings that allow population transfer within single-exciton manifolds on femtosecond timescales. Interference effects between these channels also have nontrivial effects on the resulting specta. Thus, control over exciton distributions with entangled photons could help to disentangle the relaxation pathways photosynthetic complexes utilize to convert sunlight into chemcial energy.

In an actual experiment, the PDC process provides various control knobs to tune the exciton distribution and reveal population transport dynamics within the single-exciton manifold. For example, the entanglement time varies with the length of the nonlinear medium and the pump frequency varies with the envelope of the pump pulse. If the intensity of a $|f_i\rangle$ peak increases with entanglement time T, this could suggest that intermediate single-exciton states are populated by transport within the manifold. Furthermore, decreasing the entanglement time can limit the amount of time the system spends in the single-exciton manifold and thus uncover two-exciton states that would otherwise be weakly observable with high resolution. Lastly, tuning the pump frequency to be on-resonant with a $|f_i\rangle$ state can result in oscillations due to interfering excitation pathways. On the otherhand, the lack of oscillations in an on-resonant process can reveal two-exciton states only accessible via one particular intermediate state [7].

The quantum control of excited state distributions is also particularly exciting because it is revitalizing the dream of controlling chemical reactions. Coherent control of reaction coordinates has been the holy grail of chemistry since the advent of ultrafast lasers, but initial attempts to selectively control the breaking and forming of chemical bonds proved more futile than many had hoped [8]. The quantum dynamics of molecules with even just a few atoms is much more complicated than intuition can perceive. People quickly realized that electrons were not simple localized particles, but instead delocalized charge densities in molecular orbitals, which drive chemical reactions through coordinated constructive and destructive interferences. As such, sources of photons need to reflect similar levels of complexity, which requires tunability, advanced pulse shaping techniques, and control over correlations. In a manner similar to that described above, Oka and colleagues demonstrated theoretically demonstrated that two-photon excitation using entangled photons can excite vibronic states efficiently and selectively with much stronger signal enhancement compared to a classical photon source [9]. Many other theory groups have come to similar conclusions, but the challenges of implementing such a scheme with actual molecules have so far prevented many experimentalists from confirming their predictions in any significant way. At the same time, these theory works are quite recent and it is likely only a matter of time until experiment follows.

5.2 Entangled Photon Spectroscopy of Chiral Molecules

5.2.1 Entangled Circular Dichroism

Another interesting application of entangled photons to the study of chemical systems includes the measurement of optical activity of chiral molecules. It has long been known that chiral enantiomers can be distinguished by the degree to which the polarization of an incident light is rotated upon interacting with the sample, where the rotatory dispersion relation provides information on the three-dimensional arragment of atoms within a molecule. In 2016, Tischler and colleagues measured the rotatory dispersion of sucrose enantiomers using photons with entangled spin angular momentum (SAM) [10]. In this so-called entangled circular dichroism experiment, two different states of entangled light were generated from a PDC process:

$$|\Phi_{\text{in}}\rangle = \frac{1}{\sqrt{2}}[|R,\lambda_1\rangle_1 |R,\lambda_2\rangle_2 + e^{i\alpha_0} |L,\lambda_1\rangle_1 |L,\lambda_2\rangle_2] \tag{35}$$

$$|\Psi_{\text{in}}\rangle = \frac{1}{\sqrt{2}}[|R,\lambda_1\rangle_1 |L,\lambda_2\rangle_2 + e^{i\alpha_0} |L,\lambda_1\rangle_1 |R,\lambda_2\rangle_2] \tag{36}$$

where α_0 is called the bias phase, $|P,\lambda_m\rangle_m$ indicates a photon with polarization P (R or L circularly polarized corresponding to a SAM of +1 or -1, respectively) and wavelength λ_m in path m. The optical activity experienced by light interacting with chiral molecules imparts a unitary transformation of the form $U(\alpha(C,\lambda)) = e^{-i\Lambda\alpha(C,\lambda)}$ where Λ refers to the light SAM and C is the concentration of the solution. The measurement parameters

$$\bar{\alpha} = \frac{1}{2}[\alpha(C,\lambda_1) + \alpha(C,\lambda_2)] \tag{37}$$

$$\Delta\alpha = \alpha(C,\lambda_2) + \alpha(C,\lambda_1) \tag{38}$$

were shown to relate to the coincidence counts of photons on the various detectors. For example, the HH and VV coincidences are $\frac{1}{4}(1+\cos\theta)$, whereas the HV and VH expectation values for coincidences are $\frac{1}{4}(1-\cos\theta)$ where $\theta = \alpha_0 - 4\bar{\alpha}$ when $|\Phi_{\text{in}}\rangle$ is used

and $\theta = \alpha_0 + 2\Delta\alpha$ when $|\Psi_{in}\rangle$ is used. In sum, coincidence photon counting with two different incident entangled photon states provides specific information on the mean and standard deviation of enantiomeric optical activity.

The full derivation is provided in the paper itself, but most importantly, the use of entangled light results in a factor of 2 enhancement in measurement compared to a classical scheme. Now that the principle of using entangled light to study rotatory dispersion has been established, one might envisage similar experiments with more complicated chiral molecules and nanostructures or in materials with strong spin-orbit coupling that respond differently to right- and left- circularly polarized light. For instance, the spin-valley coupling in the TMDC MoS_2 might be an interesting system to study with photons of entangled polarization since electrons at the $\pm$K points in the Brillouin zone have exclusively up or down spin, respectively. As such, spin-up electrons at say, the +K point, can only be excited into the conduction band with light of a specific SAM. Magnets might be another interesting system to study with entangled light. Circular dichroism with classical laser sources is a common method to investigate their behavior, but using entangled SAM light has so far been unreported.

5.2.2 Entangled Helical Dichroism

In the aforementioned circular dichroism experiments, the entanglement in SAM of light was used to distinguish enantiomers by interacting with magnetic dipole moments. Though light can also carry orbital angular momentum (OAM) in paraxial beams with helical wavefronts, it was previously thought that the OAM of light did not couple strongly to chiral molecules. However, Brullot and colleagues showed recently that light with OAM (nicknamed "twisted light") is in fact able to resolve molecular chirality through interactions with higher-order electric quadrupole fields (EQFs) [11]. In their experiment, light with a helical wavefront was first incident on a plasmonic nanoparticle aggregate sample synthesized in layers so as to have a polar symmetry axis. As a result of the strong EQFs created along the symmetry-broken axis, there was a measured difference in transmitted intensity in the forward and backward propogation directions due to the strong coupling of OAM to EQFs. In other words,

$$\text{Signal} = \frac{I_{\text{forward}} - I_{\text{backward}}}{\frac{I_{\text{forward}} + I_{\text{backward}}}{2}} \tag{39}$$

was nonzero. After demonstrating that helical light responds to EQFs, chiral molecules of a specific handedness were adsorbed on the nanoparticle surface and a helical dichroism signal

$$\text{Signal}_{\text{HD}} = \frac{I_+ - I_-}{\frac{I_+ + I_-}{2}} \tag{40}$$

was measured where $I_\pm$ denotes the OAM carried by the light. A measured difference in the transmission of different helicities of light was the first experimental demonstration of light's OAM ability to resolve molecular chirality (Figure 5).

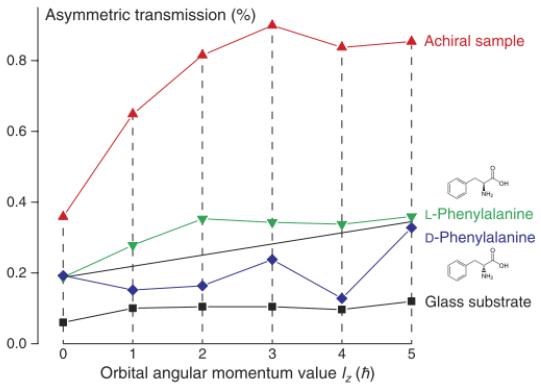

Figure 5: Plasmonic nanoparticle aggregates interact with asymmetrically with helical light giving a nonzero signal described by equation (39). L- and D-phenylalanine enantiomers respond differently to light carrying OAM with a signal described by equation (40). Reprinted from [11].

This is interesting from an entangled photon spectroscopy perspective because light with entangled OAM was first experimentally produced almost 20 years ago by the Zeilinger group [12]. What they showed was that in a type-I PDC process, in which a beam carrying OAM is converted into two entangled beams of equal polarization, OAM is conserved in the entangled photons. Mathematically, this means that if we consider that the pump beam has zero OAM, the emitted photons must be represented by the state

$$\begin{aligned} |\psi\rangle = & C_{0,0}\,|0\rangle\,|0\rangle + C_{1,-1}\,|1\rangle\,|-1\rangle + \\ & C_{-1,1}\,|-1\rangle\,|1\rangle + C_{2,-2}\,|2\rangle\,|-2\rangle + \\ & C_{-2,2}\,|-2\rangle\,|2\rangle + \ldots \end{aligned} \tag{41}$$

where the numbers in the kets indicate the OAM of the "Laguerre modes," which form a complete basis. Interestingly, this process was able to produce such a multi-mode entangled state, rather than the typical two-mode entangled state.

Applying such entangled OAM photon states towards chiral molecules might be an interesting experiment to perform. In a similar manner to the circular

dichroism experiments, one might expect such an entangled helical dichroism to determine EQF's with sub-classical noise limits. On a side note, the observation by Brullot and colleagues had that strong EQF's in nanoparticle aggregates with a polar axis couples to light carrying OAM raises the question of what effect entangled "twisted light" would have on ferroelectric materials that by definition, possess a symmetry-breaking axis. So long as the polar material possesses a large enough EQF, such an experiment might be interesting to perform.

6 Outlook

While the quantum information and physics communities have utilized quantum states of light for the past 60 or so years, their application to the fields of chemistry, biology, and materials science remains largely unexplored. The past 10 years has seen several important works by theoretical chemistry groups, investigating the light-matter interactions between entangled photons and simple molecules. However, there is still much to be explored. From the theory end, simulating spectra for complicated molecular and materials systems is a challenge and further advances in modeling many-body quantum mechanical system are important.

The unexplored experimental territory is vast and exciting. For example, entangled photon spectroscopy could offer unprecedented control of chemical reactions or photons with entangled OAM could offer insight into chemical systems for which chirality plays an important role. While simple molecular systems indeed need to be studied, entangled photons incident on low-dimensional materials would be an exciting direction to pursue in materials science. Additionally, recent efforts to generate entangled pairs of photons at x-ray wavelengths would open the door to studying atomic, molecular, and solid-state systems with atomic scale detail and core-level specificity [13]. Reliably producing entangled photons at higher energies than the optical regime would be a true accomplishment with far-reaching impacts.

In sum, chemistry, materials science, and biology are ready for quantum optics. The future is indeed exciting!

References

[1] Frank Schlawin, Konstantin E. Dorfman, and Shaul Mukamel. Entangled Two-Photon Absorption Spectroscopy. *Acc. Chem. Res.*, 51(9):2207–2214, 2018.

[2] J. G. Rarity, P. R. Tapster, E. Jakeman, T. Larchuk, R. A. Campos, M. C. Teich, and B. E.A. Saleh. Two-photon interference in a Mach-Zehnder interferometer. *Phys. Rev. Lett.*, 65(11):1348–1351, 1990.

[3] Juha Javanainen and Phillip L. Gould. Linear intensity dependence of a two-photon transition rate. *Phys. Rev. A*, 41(9):5088–5091, 1990.

[4] Frank Schlawin. Entangled photon spectroscopy. *J. Phys. B At. Mol. Opt. Phys.*, 50(20), 2017.

[5] Christopher C. Gerry and Peter L. Knight. *Introductory Quantum Optics*. Cambridge University Press, New York, 2005.

[6] Gabriela S. Schlau-Cohen, Akihito Ishizaki, Tessa R. Calhoun, Naomi S. Ginsberg, Matteo Ballottari, Roberto Bassi, and Graham R. Fleming. Elucidation of the timescales and origins of quantum electronic coherence in LHCII. *Nat. Chem.*, 4(5):389–395, 2012.

[7] Frank Schlawin, Konstantin E. Dorfman, Benjamin P. Fingerhut, and Shaul Mukamel. Suppression of population transport and control of exciton distributions by entangled photons. *Nat. Commun.*, 4:1–7, 2013.

[8] Warren S. Warren, Herschel Rabitz, and Mohammed Dahleh. Coherent control of quantum dynamics: The dream is alive. *Science (80-.).*, 259(5101):1581–1589, 1993.

[9] Hisaki Oka. Control of vibronic excitation using quantum-correlated photons. *J. Chem. Phys.*, 135(16), 2011.

[10] Nora Tischler, Mario Krenn, Robert Fickler, Xavier Vidal, Anton Zeilinger, and Gabriel Molina-Terriza. Quantum optical rotatory dispersion. *Sci. Adv.*, 2(10):1–6, 2016.

[11] Ward Brullot, Maarten K. Vanbel, Tom Swusten, and Thierry Verbiest. Resolving enantiomers using the optical angular momentum of twisted light. *Sci. Adv.*, 2(3):1–6, 2016.

[12] Alois Mair, Alipasha Vaziri, Gregor Weihs, and Anton Zeilinger. Entanglement of the orbital angular momentum states of photons. *Nature*, 412:313–316, 2001.

[13] S. Sofer, E. Strizhevsky, A. Schori, K. Tamasaku, and S. Shwartz. Quantum Enhanced X-ray Detection. *Phys. Rev. X*, 9(3):1–6, 2019.